*Int. J. Therm. Sci.* (2001) 40, 195–204

S1290-0729(00)01208-4/FLA

# Numerical study of the performance of a church window tube bundle condenser

Inés Suárez Ramón, Manuela Prieto González *

*University of Oviedo, Energy Department, Campus de Viesques, Ctra. de Villaviciosa, s/n, 33204 Gijón, Asturias, Spain*

(Received 11 August 1999, accepted 7 March 2000)

**Abstract** — Two steam surface condenser design methods are compared: that of the Heat Exchange Institute Standards and a three-dimensional steady-state numerical model for simulating the flow, the heat and the mass transfer in this type of industrial equipment. In the numerical model, the study of the shell flow is carried out using a single-phase approach, the presence of the tubes is simulated through the porosity factor, and the heat and mass transfer processes are modelled using empirical correlations. The variables condenser pressure and overall heat transfer coefficient are analysed applying both methods. The influence on these variables of the steam mass flow rate from the turbine exhaust, the venting outlet pressure, the tube cleanliness factor, the inlet water temperature, and the water velocity is studied. The overall heat transfer coefficient is under-predicted with the numerical model, its value being 4.5–8.5 % lower than that obtained using the Heat Exchange Institute Standards method. © 2001 Éditions scientifiques et médicales Elsevier SAS

**condenser performance / steam surface condenser / numerical modelling / condensation / noncondensable gases**

## Nomenclature

| | | |
|---|---|---|
| $A$ | total heat transfer area | $m^2$ |
| $Cp$ | specific heat at constant pressure | $J{\cdot}kg^{-1}{\cdot}K^{-1}$ |
| $D_i$ | inner diameter of tubes | m |
| $D_o$ | outer diameter of tubes | m |
| $D_{sa}$ | diffusivity of steam in air | $m^2{\cdot}s^{-1}$ |
| $\boldsymbol{F}$ | flow resistance force per unit volume due to the tube bundle | $N{\cdot}m^{-3}$ |
| $F_C$ | tube cleanliness factor | |
| $F_M$ | correction factor for material and tube gauge | |
| $F_W$ | correction factor for inlet water temperature | |
| $H$ | Ackerman's correction coefficient | |
| $h$ | heat transfer coefficient | $W{\cdot}m^{-2}{\cdot}K^{-1}$ |
| $i$ | specific enthalpy | $J{\cdot}kg^{-1}$ |
| $k$ | thermal conductivity of tubes | $W{\cdot}m^{-1}{\cdot}K^{-1}$ |
| LMTD | logarithmic mean temperature difference | K |
| $m$ | mass flow rate | $kg{\cdot}s^{-1}$ |
| $m_a$ | mass flow rate per unit area | $kg{\cdot}s^{-1}{\cdot}m^{-2}$ |
| $m_v$ | mass flow rate per unit volume | $kg{\cdot}s^{-1}{\cdot}m^{-3}$ |
| $N$ | total number of control volumes | |
| $P$ | pressure | Pa |
| $Pt$ | tube pitch | m |
| $Q$ | heat transfer rate | W |
| $q_a$ | heat transfer rate per unit area | $W{\cdot}m^{-2}$ |
| $q_v$ | heat transfer rate per unit volume | $W{\cdot}m^{-3}$ |
| $R$ | thermal resistance $= 1/U$ | $m^2{\cdot}K{\cdot}W^{-1}$ |
| $R_f$ | fouling resistance | $m^2{\cdot}K{\cdot}W^{-1}$ |
| $T$ | temperature | °C |
| $\boldsymbol{u}$ | velocity vector | $m{\cdot}s^{-1}$ |
| $u$ | velocity | $m{\cdot}s^{-1}$ |
| $U$ | overall heat transfer coefficient | $W{\cdot}m^{-2}{\cdot}K^{-1}$ |
| $U_1$ | uncorrected overall heat transfer coefficient | $W{\cdot}m^{-2}{\cdot}K^{-1}$ |
| $V$ | volume | $m^3$ |
| $Y_a$ | air mass fraction | |

*Greek symbols*

| | | |
|---|---|---|
| $\beta$ | volumetric porosity factor | |
| $\varepsilon_P$ | relative error of pressure $= \lvert(P_{NM} - P_{SSSC})/P_{SSSC}\rvert{\cdot}100$ | % |
| $\varepsilon_U$ | relative error of overall heat transfer coefficient $= \lvert(U_{NM} - U_{SSSC})/U_{SSSC}\rvert{\cdot}100$ | % |
| $\rho$ | density | $kg{\cdot}m^{-3}$ |

* Correspondence and reprints.
*E-mail address:* manuelap@correo.uniovi.es (M.P. González).

| | | |
|---|---|---|
| $\mu_{\text{eff}}$ | effective dynamic viscosity of the mixture $= \mu_{\text{L}} + \mu_{\text{T}}$ . . . . . | $\text{N}\cdot\text{m}^{-2}\cdot\text{s}^{-1}$ |
| $\mu_{\text{L}}$ | laminar dynamic viscosity of the mixture . . . . . | $\text{N}\cdot\text{m}^{-2}\cdot\text{s}^{-1}$ |
| $\mu_{\text{T}}$ | turbulent dynamic viscosity of the mixture $= 20\ \mu_{\text{L}}$ . . . . . | $\text{N}\cdot\text{m}^{-2}\cdot\text{s}^{-1}$ |

*Subscripts*

| | |
|---|---|
| avg | average value |
| c | condensate |
| cc | corrected condensate |
| f | fouling |
| g | gas (steam–air mixture) |
| i | inlet |
| if | mixture–condensate interface |
| $j$ | index |
| lg | liquid–gas change |
| NM | numerical model |
| o | outlet |
| s | steam |
| SSSC | "Standards for Steam Surface Condensers" |
| w | water |
| $x, y, z$ | coordinates |

## 1. INTRODUCTION

The design of thermal power plant condensers has traditionally been based on recommendations elaborated by condenser manufacturers founded on previous designs, and expensive experimental tests. In "Standards for Steam Surface Condensers" (SSSC) developed by the Heat Exchange Institute (HEI) [1], the following equations (1)–(4) are proposed for condenser design. The heat transfer rate in the condenser, the saturation pressure, the water mass flow rate and the inlet water temperature are required to solve these equations. The condensate mass flow rate, the outlet water temperature, and the total heat transfer area are calculated, together with the definition of the arrangement, the material and the geometric parameters of the tubes:

$$Q = m_{\text{c}} i_{\text{lg}} \tag{1}$$

$$Q = m_{\text{w}} Cp_{\text{w}} (T_{\text{w,o}} - T_{\text{w,i}}) \tag{2}$$

$$Q = U A \frac{T_{\text{w,o}} - T_{\text{w,i}}}{\ln((T_{\text{g}} - T_{\text{w,i}})/(T_{\text{g}} - T_{\text{w,o}}))} \tag{3}$$

$$U = U_1 F_{\text{W}} F_{\text{M}} F_{\text{C}} \tag{4}$$

where $Q$ is the heat transfer rate in the condenser, $m_{\text{c}}$ is the condensate mass flow rate, $i_{\text{lg}}$ is the steam vaporisation specific enthalpy, $m_{\text{w}}$ is the water mass flow rate, $Cp_{\text{w}}$ is the specific heat at constant pressure of the water evaluated at the average water temperature between the inlet and the outlet, $T_{\text{w,o}}$ is the outlet water temperature, $T_{\text{w,i}}$ is the inlet water temperature, $U$ is the overall heat transfer coefficient, $A$ is the total heat transfer area, $T_{\text{g}}$ is the mixture temperature calculated as the saturation temperature corresponding to the steam pressure, $U_1$ is the uncorrected overall heat transfer coefficient, $F_{\text{W}}$ is the correction factor for the inlet water temperature, $F_{\text{M}}$ is the correction factor for the material and tube gauge and $F_{\text{C}}$ is the tube cleanliness factor.

The SSSC does not take into account a number of factors that affect the condenser pressure and the overall heat transfer coefficient: the presence of noncondensable gases mixed with the steam, inundation of the tubes by the condensing steam, the pressure loss of the mixture across the tube bundle, the geometry of the tube bundle, and the design of the noncondensable gases extraction equipment.

There is a considerable number of numerical models for simulating the performance of steam surface condensers [2–9], which give detailed information on the distribution of the mixture velocity, the mixture pressure, the concentration of noncondensable gases, and the water temperature. These numerical models represent a very useful tool for studying the processes inside the condensers, and for investigating the effect of alternative geometries more quickly and cheaply than experimental studies, with a reduced number of tests. Most of the models assume two-dimensional performance, and use a single-phase approach to study the flow within the shell. The thermal effects of steam condensation, heat and mass transfer from the mixture to the condensate at the interface, steam shear at the interface, inundation of the tubes by the condensing steam, and pressure loss of the mixture across the tube bundle are modelled through empirical correlations. The effect of tube fouling is included as an additional thermal resistance to the heat transfer, which could be quite substantial depending on the quality of the water, particularly in condensers working with seawater as coolant. The performance of this type of model has been experimentally assessed in [2, 8, 9].

In the present study, a numerical model is described that is based on equivalent assumptions to those mentioned above, but which considers the flow inside the shell as three dimensional, using an approach based on the Colburn–Hougen model [10] and empirical correlations for convective heat transfer coefficients. The model was applied to a feedwater heater from a thermal power plant, and the numerical results were found to be satisfactory compared with design and experimental data in [11].

The focus of the study is now to compare the results of the SSSC with those obtained using the numerical model (NM), since there are no existing bibliographic references in this field. Both methods are applied to a single-pass condenser with a church window tube bundle. The comparison is based on the analysis of two variables: the condenser pressure and the overall heat transfer coefficient. The evolution of the variables is studied with respect to five parameters: the steam mass flow rate from the turbine exhaust, the venting outlet pressure, the tube cleanliness factor, the inlet water temperature, and the water velocity. Moreover, the differences between the values of the variables obtained using both methods are quantified.

## 2. NUMERICAL MODEL

### 2.1. Description

The numerical model simulates the steady-state flow and the heat and mass transfer processes in thermal power plant condensers.

The shell-fluid is a mixture of steam and noncondensable gases, mainly air. The flow within the shell is simulated using a single-phase approach, assuming that the condensate disappears from the domain as it is formed.

The tube-fluid is cooling water. As the flow pattern is known, the water velocity along the tubes is considered constant, and it is not necessary to obtain the water velocity field.

The conservation equations of the mixture mass (5), the mixture momentum (6), the air mass (7), and the water energy (8) are solved in each control volume:

$$\operatorname{div}(\beta\rho_{\mathrm{g}}\boldsymbol{u}_{\mathrm{g}}) = -\beta m_{\mathrm{c,v}} \tag{5}$$

$$\operatorname{div}\big(\beta\rho_{\mathrm{g}}(\boldsymbol{u}_{\mathrm{g}}\otimes\boldsymbol{u}_{\mathrm{g}})\big) = \operatorname{div}\big(\beta\mu_{\mathrm{eff}}\operatorname{grad}(\boldsymbol{u}_{\mathrm{g}})\big) - \beta\operatorname{grad}(P_{\mathrm{g}}) - \beta\boldsymbol{F} - \beta m_{\mathrm{c,v}}\boldsymbol{u}_{\mathrm{g}} \tag{6}$$

$$\operatorname{div}(\beta\rho_{\mathrm{g}}\boldsymbol{u}_{\mathrm{g}}Y_{\mathrm{a}}) = \operatorname{div}\big(\beta\rho_{\mathrm{g}}D_{\mathrm{sa}}\operatorname{grad}(Y_{\mathrm{a}})\big) \tag{7}$$

$$\operatorname{div}(\rho_{\mathrm{w}}\boldsymbol{u}_{\mathrm{w}}i_{\mathrm{w}}) = q_{\mathrm{v}} \tag{8}$$

where $\beta$ is the porosity factor, $\rho_{\mathrm{g}}$ is the mixture density, $\boldsymbol{u}_{\mathrm{g}}$ is the mixture velocity, $m_{\mathrm{c,v}}$ is the condensate mass flow rate per unit volume, $\mu_{\mathrm{eff}}$ is the effective dynamic viscosity of the mixture, $P_{\mathrm{g}}$ is the mixture pressure, $\boldsymbol{F}$ is the flow resistance force due to the tube bundle, $Y_{\mathrm{a}}$ is the air mass fraction, $D_{\mathrm{sa}}$ is the diffusivity of steam in air, $\rho_{\mathrm{w}}$ is the water density, $\boldsymbol{u}_{\mathrm{w}}$ is the water velocity, and $q_{\mathrm{v}}$ is the heat transfer rate per unit volume.

The tube bundle is simulated using the volumetric porosity factor, which is defined as the ratio of the volume occupied by the shell-side fluid and the total volume. It is given by equation (9) for a staggered arrangement of tubes at 60°:

$$\beta = 1 - \frac{\pi}{2\sqrt{3}}\left(\frac{D_{\mathrm{o}}}{Pt}\right)^2 \tag{9}$$

where $\beta$ is the volumetric porosity factor, $D_{\mathrm{o}}$ is the outer diameter of the tubes, and $Pt$ is the tube pitch.

The turbulence within the shell is modelled through the effective dynamic viscosity, which is defined as the sum of the laminar and turbulent dynamic viscosities. In the present study, the turbulent dynamic viscosity is defined as 20 times the laminar dynamic viscosity, in accordance with the sensitivity analysis carried out in prior studies [8, 9, 12].

The condensate mass flow rate is taken into account in the conservation equations of the mixture mass and momentum as source terms, which represent mass and momentum sinks.

The friction force in the source term of the momentum conservation equation is modelled using adequate empirical correlations for crossflow and longitudinal flow as a function of geometric parameters of the tubes, friction factors, and physical properties of the mixture. The expressions in [5, 8, 9] are used for calculating the crossflow components, and the internal flow expression is employed for evaluating the longitudinal component.

The study of the heat and mass transfer is carried out according to Colburn and Hougen's film theory [12], taking into account the thermal resistance of the water inside the tubes, the wall of the tubes, the condensate film, tube fouling, and the gaseous mixture, as well as the vaporisation heat transfer rate. Equation (10) is solved in each control volume to obtain the temperature at the mixture–condensate interface:

$$q_a = \frac{T_{\mathrm{if}} - T_{\mathrm{w}}}{\frac{D_{\mathrm{o}}}{D_{\mathrm{i}}}\frac{1}{h_{\mathrm{w}}} + \frac{D_{\mathrm{o}}}{2k}\ln\left(\frac{D_{\mathrm{o}}}{D_{\mathrm{i}}}\right) + \frac{1}{h_{\mathrm{cc}}} + R_{\mathrm{f,NM}}} = h_{\mathrm{g}}\frac{H}{1-\mathrm{e}^{-H}}(T_{\mathrm{g}} - T_{\mathrm{if}}) + i_{\mathrm{lg}}m_{\mathrm{c,a}} \tag{10}$$

where $q_{\mathrm{a}}$ is the heat transfer rate per unit area, $T_{\mathrm{if}}$ is the temperature at the mixture–condensate interface, $T_{\mathrm{w}}$ is the water temperature, $D_{\mathrm{i}}$ is the inner diameter of the tubes, $h_{\mathrm{w}}$ is the water-side heat transfer coefficient, $k$ is the thermal conductivity of the tubes, $h_{\mathrm{cc}}$ is the

condensate film heat transfer coefficient corrected by the condensate inundation of the tubes factor and the steam shear at the interface factor, $R_{f,NM}$ is the tube fouling thermal resistance, $h_g$ is the heat transfer coefficient of the mixture, $H$ is Ackerman's correction factor, $i_{lg}$ is the vaporisation specific enthalpy of steam, and $m_{c,a}$ is the condensate mass flow rate per unit area.

The water-side heat transfer coefficient is calculated using the Dittus–Boelter correlation given in [13].

The condensate film heat transfer coefficient is calculated from Nusselt's correlation [14], and is corrected using two factors to take into account the effects of the condensate inundation of the tubes [15], and the steam shear at the interface [14].

The heat transfer coefficient of the mixture is evaluated from the correlation proposed by Taborek [16], and is corrected with Ackerman's factor [17] to take into account the diffusion effects due to the presence of air mixed with the steam.

## 2.2. Application

The three-dimensional numerical model is applied to a condenser with a horizontal tube bundle. *Figure 1*(*a*) shows a cross section of the condenser. The steam from the turbine exhaust enters the condenser at the top of the shell and flows across the tubes to the bundle centre area due to the vacuum produced by the venting equipment, which extracts the noncondensable gases and the noncondensed steam. The mixture passes to the venting conduct through a set of orifices of very small diameter uniformly distributed along the conduct. The aluminum brass tubes are in a staggered arrangement at 60°, 9.75 m long, 0.024 m outer diameter, and 18 BWG gauge.

The geometry and the boundary conditions are symmetrical with respect to the $y$-direction and only one half is simulated. The Cartesian grid used is 0.1 m in size, except in the baffles and venting area, where a refined grid is defined to approximate the baffle shape, and to take into account the small dimension of the venting area. The resulting grid is $23 \times 87 \times 120$ control volumes, and a tube bundle cross section is shown in *figure 1*(*b*).

The boundary conditions defined are the following: the steam and air mass flow rates in the shell inlet, the water velocity and temperature in the tube inlet, and the venting outlet pressure.

The operating conditions are indicated in *table I*. The air mass flow rate in the condenser is assumed to be constant. Three values are chosen for each of the parameters: the steam mass flow rate, the noncondensable gases outlet pressure, the tube cleanliness factor, the inlet

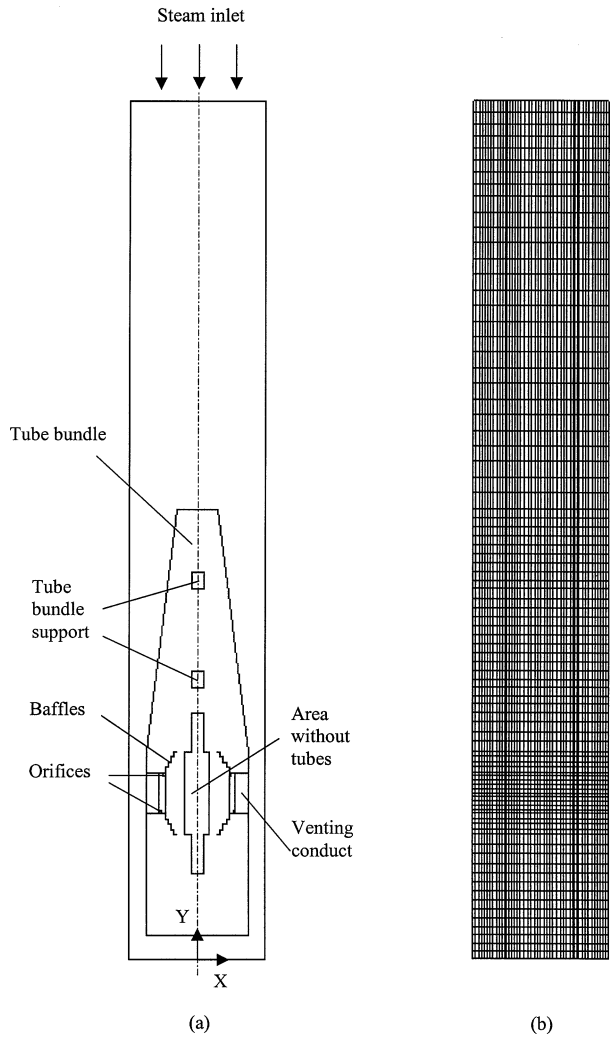


**Figure 1.** (a) Geometry of the condenser, (b) grid.

TABLE I
Performance conditions.

| | | | |
|---|---|---|---|
| Constant data | | | |
| Air mass flow rate ($kg \cdot s^{-1}$) | $5.56 \cdot 10^{-4}$ | | |
| Variable data | | | |
| Steam mass flow rate ($kg \cdot s^{-1}$) | 30.84 | 23.73 | 16.95 |
| Venting outlet pressure (Pa) | 2 800 | 3 200 | 3 800 |
| Tube cleanliness factor (dimensionless) | 0.6 | 0.8 | 1 |
| Inlet water temperature (K) | 287.15 | 291.15 | 295.15 |
| Water velocity ($m \cdot s^{-1}$) | 1.5 | 1.8 | 2.1 |

water temperature, and the water velocity. These values give a sufficiently wide range of the condenser operating conditions.

## 3. ANALYSIS OF THE MODELS

In the present study, the methods are applied to a condenser for which the total heat transfer area, the geometry, the arrangement, the material and the geometric parameters of the tubes are known.

For the application of the SSSC to each set of operating conditions, the values of the following variables are required: the tube cleanliness factor, the water mass flow rate, which is calculated from the values of $T_{w,i}$ and $u_w$, and the heat transfer rate in the condenser, the value of which has been assumed to be equal to the value obtained using the numerical model for the comparison of the results of both methods. Equations (1)–(4) are solved and the condenser pressure, the overall heat transfer coefficient, the condensate mass flow rate, and the outlet water temperature are obtained.

For the application of the numerical model to each set of operating conditions, the values of the boundary conditions and the tube fouling thermal resistance are required. By solving equations (5)–(10), the distributions of the mixture velocity, the condenser pressure, the air mass fraction, the water and mixture temperatures, the heat transfer rate per unit volume, and the condensate mass flow rate per unit volume are obtained. From these results, the overall heat transfer coefficient, the total heat transfer rate in the condenser, the total condensate mass flow rate, and the average outlet water temperature are calculated.

For the comparison of both methods, a tube fouling thermal resistance, $R_{f,NM}$, is defined for the numerical model in accordance with the value of $F_C$ used in the SSSC. This thermal resistance is calculated from equation (11) as the difference between the fouling thermal resistance of a tube, the area of which is equal to the total heat transfer area of the condenser, for a known cleanliness factor, $R_f(F_C)$, and the fouling thermal resistance of this tube for a cleanliness factor equal to 1, $R_f(F_C = 1)$. Thus, the fouling thermal resistance is equal to zero for clean tubes ($F_C = 1$) and increases when the cleanliness factor decreases:

$$R_{f,NM} = R_f(F_C) - R_f(F_C = 1) \tag{11}$$

The fouling thermal resistance of the tube is calculated assuming that the heat transfer rate in the tube is equal to the heat transfer rate in the condenser. The former is obtained through equation (12), and the latter is calculated solving equations (1)–(4) from the values of $m_c$, $F_C$, $T_{w,i}$ and $u_w$, assuming that the total steam mass flow rate condenses. The value of $m_c$ is equal to the steam mass flow rate used in the numerical model:

$$Q = \frac{1}{\frac{D_o}{D_i}\frac{1}{h_w} + \frac{D_o}{2k}\ln\left(\frac{D_o}{D_i}\right) + \frac{1}{h_c} + R_f(F_C)} A(T_g - T_{w,avg})$$

$$T_{w,avg} = \frac{T_{w,i} + T_{w,o}}{2} \tag{12}$$

With regard to the numerical model results, the total heat transfer rate in the condenser and the total condensate mass flow rate are calculated as the sum of the values obtained in each control volume from equations (13) and (14). The average value of the outlet water temperature is calculated from the average value of the water outlet specific enthalpy defined by equation (15):

$$Q = \frac{\sum_{j=1}^{N} q_{v,j} V_j}{\sum_{j=1}^{N} V_j} \tag{13}$$

$$m_c = \frac{\sum_{j=1}^{N} m_{c,v,j} V_j}{\sum_{j=1}^{N} V_j} \tag{14}$$

where $q_{v,j}$ is the heat rate per unit volume transferred in the control volume $j$, $m_c$ is the condensate mass flow rate, $m_{c,v,j}$ is the condensate mass flow rate per unit volume in the control volume $j$, and $V_j$ is the volume of the control volume $j$;

$$i_{w,o,avg} = \frac{\sum_{j=1}^{N} i_{w,j} m_{w,j}}{\sum_{j=1}^{N} m_{w,j}} = \int_{273.15}^{T_{w,o,avg}} Cp_w(T)\,dT \tag{15}$$

where $i_{w,o}$ is the average outlet water specific enthalpy, $i_{w,j}$ is the average water specific enthalpy in the control volume $j$, $m_{w,j}$ is the water mass flow rate in the control volume $j$, and $T_{w,o,avg}$ is the average outlet water temperature.

With respect to the condenser pressure distribution, the SSSC assume a single value for each set of operating conditions, defined as the pressure maintained within the condenser shell at locations no more than 0.3 m from the first tube ($P_{SSSC}$). *Figure 2* shows the pressure distribution obtained using the numerical model in two cross sections of the condenser, one situated near the water inlet, *figure 2(a)*, and the other placed near the water outlet, *figure 2(b)*. It can be observed that the pressure is maximum at the mixture inlet, and decreases as the mixture comes across the tubes to the venting outlet, where the pressure is minimum. Moreover, the

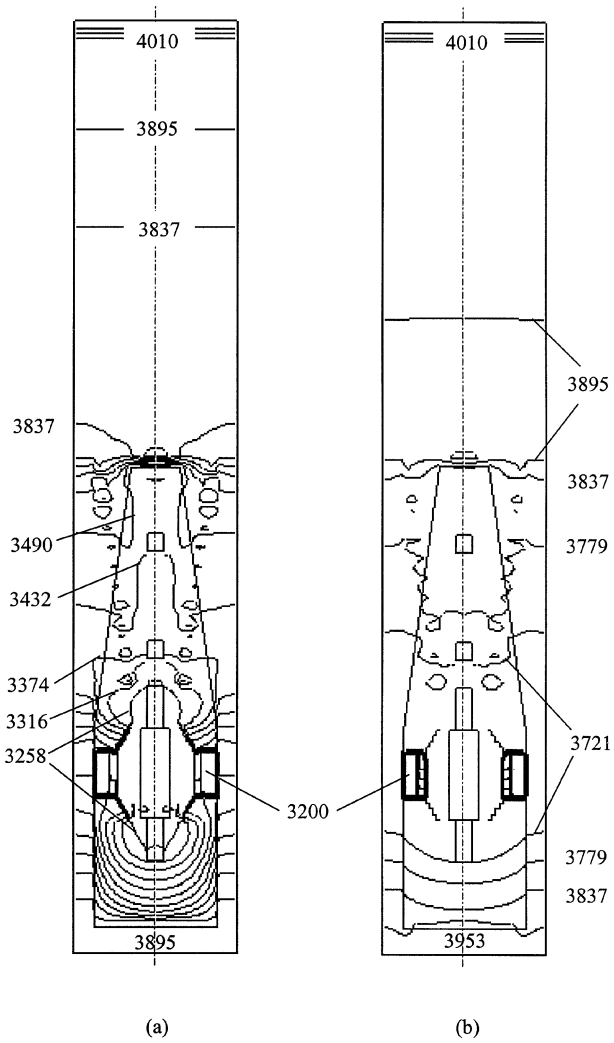


**Figure 2.** Distribution of the condenser pressure obtained with the numerical model (Pa): (a) $XY$ plane at water inlet, (b) $XY$ plane at water outlet.

pressure increases along the tubes as the water heats up, being higher at the water outlet than at the water inlet. Therefore, it is essential to define a criterion for the condenser pressure of the numerical model so as to be able to compare both methods, as the SSSC do not define the measurement point exactly. In the present study, the pressure in the control volume located in the cross section of the tube bundle situated at the middle of the tube length, on the condenser symmetry axis, and 0.05 m above the first tube row, is defined as the condenser pressure of the numerical model ($P_{NM}$), according to the SSSC.

The overall heat transfer coefficient of the numerical model ($U_{NM}$) is calculated from equation (3) from the saturation temperature at pressure $P_{NM}$, and is compared with the overall heat transfer coefficient obtained using the SSSC, $U_{SSSC}$.

## 4. RESULTS

### 4.1. Condenser pressure

*Figure 3* shows the variation of $P_{SSSC}$ and $P_{NM}$ versus $u_w$ for $m_s = 30.84$ kg·s$^{-1}$ and $P_{g,o} = 3\,200$ Pa, varying the values of $F_C$ and $T_{w,i}$. It is observed that $P_{NM}$ is greater than $P_{SSSC}$ in every case, both pressures decreasing when $u_w$ and $F_C$ increase, and when $T_{w,i}$ decreases.

In most cases, the difference in pressure between both methods presents little variation with respect to the parameters $F_C$, $T_{w,i}$ and $u_w$. However, in the cases corresponding to low values of $T_{w,i}$ and high values of $F_C$, $P_{NM}$ is observed to behave differently, due to the value of $P_{g,o}$ chosen for the numerical simulations. *Figure 4* shows the variation curves of $P_{SSSC}$ and $P_{NM}$ versus $u_w$ for $m_s = 30.84$ kg·s$^{-1}$, $F_C = 1.0$ and $T_{w,i} = 14$ °C, and for six different values of $P_{g,o}$. While the calculation method of $P_{SSSC}$ does not depend on $P_{g,o}$, this parameter does affect the value of $P_{NM}$. Decreasing the value of $P_{g,o}$, the variation curves of $P_{SSSC}$ and $P_{NM}$ have a similar slope, and the difference between the pressures obtained using both methods decreases. Moreover, there is a value of $P_{g,o}$ (around 2 600 Pa in this case) below which the pressure of the numerical model is considered independent of the said parameter. It was observed in later simulations that this value of $P_{g,o}$ increases with the value of $T_{w,i}$.

With regard to the variation of the condenser pressure with the value of the steam mass flow rate, *table II* presents the results obtained using both methods for $T_{w,i} = 22$ °C, $u_w = 1.8$ m·s$^{-1}$, and three different values of $m_s$, $P_{g,o}$ and $F_C$, as well as the relative error of pressure of the numerical model with respect to the SSSC. It can be seen that the relative error and the values of $P_{SSSC}$ and $P_{NM}$ decrease with the value of the steam mass flow rate, since the heat transfer rate and the cooling water mass flow rate are constant in each case.

### 4.2. Overall heat transfer coefficient

*Figure 5* shows the variation of $U_{SSSC}$ and $U_{NM}$ versus $u_w$ for $m_s = 30.84$ kg·s$^{-1}$ and $P_{g,o} = 3\,200$ Pa, varying

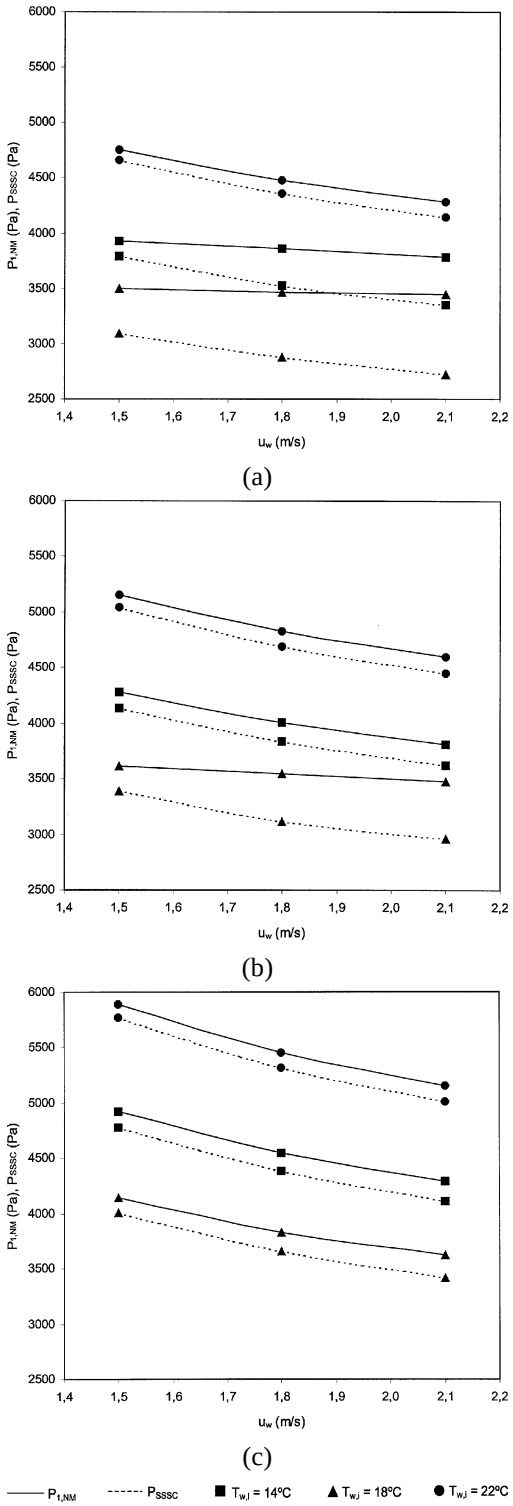


**Figure 3.** Variation of the condenser pressure with $P_{g,o}$, $T_{w,i}$ and $u_w$: $m_s = 30.84$ kg·s$^{-1}$, (a) $F_C = 1.0$, (b) $F_C = 0.8$, and (c) $F_C = 0.6$.

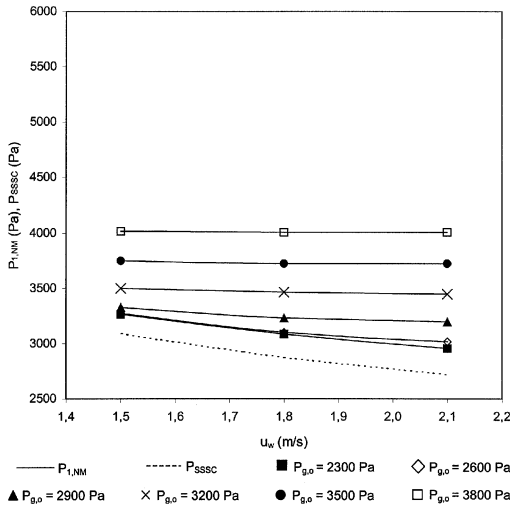


**Figure 4.** Variation of the condenser pressure with $P_{g,o}$ and $u_w$: $m_s = 30.84$ kg·s$^{-1}$, $F_C = 1.0$, $T_{w,i} = 14$ °C.

TABLE II
Comparison of the condenser pressure ($T_{w,i} = 22$ °C, $u_w = 1.35$ m·s$^{-1}$).

| Parameters | | | Condenser pressure (Pa) | | Relative error (%) |
|---|---|---|---|---|---|
| $m_s$ (kg·s$^{-1}$) | $P_{g,o}$ (Pa) | $F_C$ | $P_{NM}$ | $P_{SSSC}$ | $\varepsilon_P$ |
| 30.84 | 3800 | 1.0 | 4970 | 4658 | 2.70 |
| 30.84 | 3800 | 0.8 | 5371 | 5001 | 2.72 |
| 30.84 | 3800 | 0.6 | 6087 | 5642 | 2.50 |
| 23.73 | 3200 | 1.0 | 4331 | 4100 | 2.16 |
| 23.73 | 3200 | 0.8 | 4607 | 4335 | 2.37 |
| 23.73 | 3200 | 0.6 | 5091 | 4769 | 2.39 |
| 16.95 | 2800 | 1.0 | 3775 | 3621 | 1.36 |
| 16.95 | 2800 | 0.8 | 3952 | 3772 | 1.66 |
| 16.95 | 2800 | 0.6 | 4258 | 4046 | 1.86 |

the values of $F_C$ and $T_{w,i}$. It is observed that $U_{NM}$ is lower than $U_{SSSC}$ in every case, both coefficients increasing when $F_C$ increases and $T_{w,i}$ decreases.

With respect to the variation of the overall heat transfer coefficient with $u_w$, both coefficients increase, in the majority of cases, with the value of $u_w$, the slope of the curve of $U_{SSSC}$ being generally greater than that of $U_{NM}$. However, in the same cases as those observed in the pressure analysis, $U_{NM}$ decreases for high values of $u_w$. This unexpected behaviour of $U_{NM}$ is caused by the value of $P_{g,o}$ chosen for the numerical simulations. The influence of $P_{g,o}$ on the overall heat transfer coefficient was studied in a similar way to that of the pressure analysis. *Figure 6* shows the variation curves of $U_{SSSC}$ and $U_{NM}$ versus $u_w$ for $m_s = 30.84$ kg·s$^{-1}$,

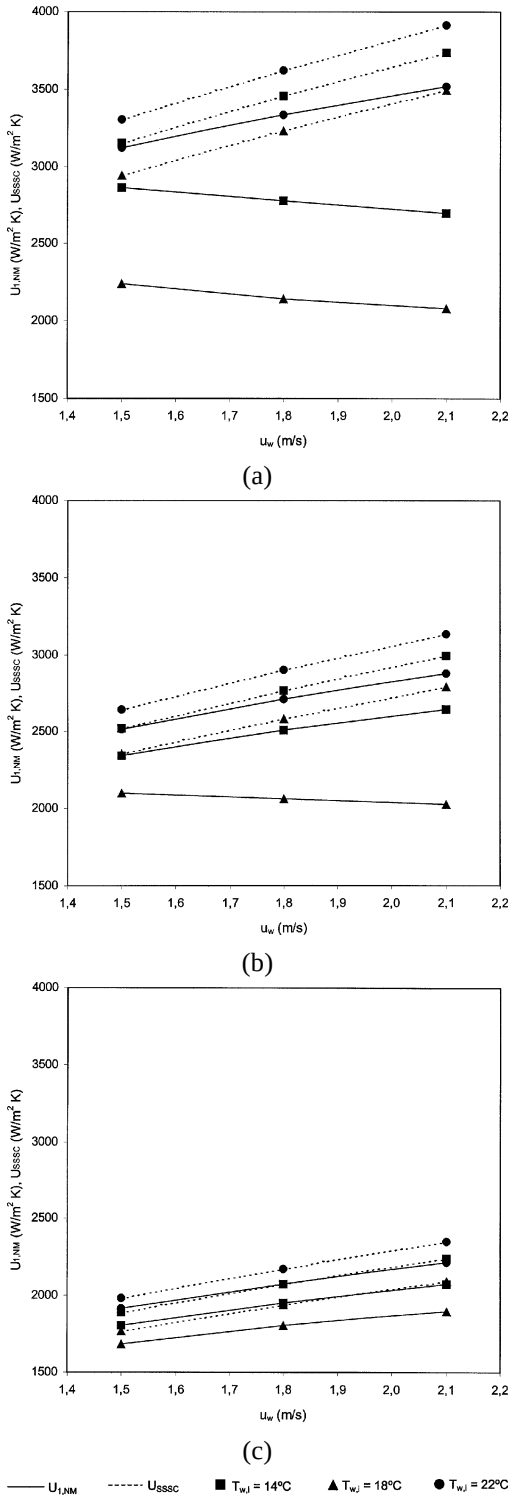


**Figure 5.** Variation of the overall heat transfer coefficient with $P_{g,o}$, $T_{w,i}$ and $u_w$: $m_s = 30.84$ kg·s$^{-1}$, (a) $F_C = 1.0$, (b) $F_C = 0.8$, and (c) $F_C = 0.6$.

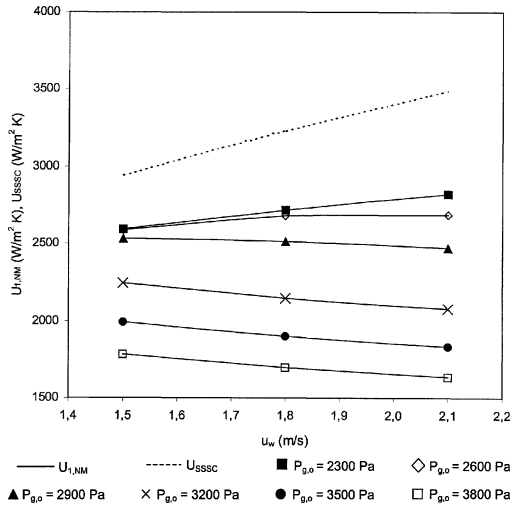


**Figure 6.** Variation of the overall heat transfer coefficient with $P_{g,o}$ and $u_w$: $m_s = 30.84$ kg·s$^{-1}$, $F_C = 1.0$, $T_{w,i} = 14$ °C.

TABLE III
Comparison of the overall heat transfer coefficient ($T_{w,i} = 22$ °C, $u_w = 1.35$ m·s$^{-1}$).

| Parameters | | | Overall heat transfer coefficient (W·m$^{-2}$·K$^{-1}$) | | Relative error (%) |
|---|---|---|---|---|---|
| $m_s$ (kg·s$^{-1}$) | $P_{g,o}$ (Pa) | $F_C$ | $U_{NM}$ | $U_{SSSC}$ | $\varepsilon_U$ |
| 30.84 | 3800 | 1.0 | 2960.1 | 3615.1 | 8.0 |
| 30.84 | 3800 | 0.8 | 2429.1 | 2892.1 | 6.5 |
| 30.84 | 3800 | 0.6 | 1885.4 | 2169.1 | 4.6 |
| 23.73 | 3200 | 1.0 | 2918.3 | 3615.1 | 8.2 |
| 23.73 | 3200 | 0.8 | 2396.5 | 2892.1 | 7.2 |
| 23.73 | 3200 | 0.6 | 1863.1 | 2169.1 | 5.5 |
| 16.95 | 2800 | 1.0 | 2894.6 | 3615.1 | 7.1 |
| 16.95 | 2800 | 0.8 | 2375.1 | 2892.1 | 6.9 |
| 16.95 | 2800 | 0.6 | 1845.5 | 2169.1 | 5.9 |

$F_C = 1.0$ and $T_{w,i} = 14$ °C, and for six different values of $P_{g,o}$. While the calculation method of $U_{SSSC}$ does not depend on $P_{g,o}$, this parameter does affect the value of $U_{NM}$. Decreasing the value of $P_{g,o}$, the slope of the curves of $U_{NM}$ increases and its sign changes from negative to positive, decreasing the differences between both methods. Moreover, there is a value of $P_{g,o}$ (the same as observed in the pressure analysis) below which the overall heat transfer coefficient of the numerical model is considered independent of the said parameter.

In relation to the variation of the overall heat transfer coefficient with the value of the steam mass flow rate, *table III* presents the results obtained using both methods for $T_{w,i} = 22$ °C, $u_w = 1.8$ m·s$^{-1}$, and three different values of $m_s$, $P_{g,o}$ and $F_C$, as well as the relative error

of the numerical model with respect to the SSSC. It can be seen that the values of $U_{SSSC}$ and $U_{NM}$ decrease with the value of the steam mass flow rate, while the relative error is almost constant.

## 5. CONCLUSIONS

In the present study, the variables *condenser pressure* and *overall heat transfer coefficient* obtained using the "Standards for Steam Surface Condensers" (SSSC) of the Heat Exchange Institute and a three-dimensional numerical model were compared. The comparison was carried out from two different points of view: the evolution of the variables with five parameters (the steam mass flow rate from the turbine exhaust, the venting outlet pressure, the tube cleanliness factor, the inlet water temperature, and the water velocity), as well as the quantification of the differences between the values obtained using both methods.

As expected, both in the numerical model and in the SSSC, the condenser pressure decreases and the overall heat transfer coefficient increases when the heat transfer processes in the condenser are improved due to the variation of certain parameters. In particular, this tendency appears when there is an increment in the water velocity, and when the tube cleanliness factor or the inlet water temperature decreases. With respect to the steam mass flow rate, the condenser pressure and the overall heat transfer coefficient obtained using both methods decrease with this parameter.

Tendencies differing from this overall performance, which are observed in the numerical results for low values of the inlet water temperature and high values of the tube cleanliness factor, are corrected by decreasing the value of the venting outlet pressure.

In spite of the similar overall behaviour of the methods, there are some differences between the values of the condenser pressure and the overall heat transfer coefficient obtained using both methods. The numerical model predicts higher condenser pressures and lower overall heat transfer coefficients than the SSSC. Consequently, the analysis of the condenser performance will be more conservative using the numerical model than that of the SSSC, and the design of condensers with the numerical model will lead to larger equipment than that obtained using the SSSC method, a conclusion that is contrast with the logical thought that simplified engineering calculation methods adopt a certain degree of conservatism, being used only for gross estimates. There are two main reasons for this conclusion: on the one hand, the SSSC do not take into account certain negative effects that aggravate the heat and mass transfer in the condensers, mainly the inundation of the tubes by the condensate and the presence of noncondensable gases mixed with the steam. On the other hand, the details concerning the performance conditions and the geometries to which the SSSC could be satisfactory applied are very poor.

With regards to the steam mass flow rate, the differences between the condenser pressures obtained using both methods decrease with this parameter, while the differences between the overall heat transfer coefficients are almost constant. The reason is that when the steam mass flow rate decreases and the values of the heat transfer rate and the cooling water mass flow rate are maintained constant, the pressure predicted by the numerical model decreases, approaching the pressure predicted by that of the SSSC, but satisfactorily predicting the overall heat transfer coefficient.

The conclusions of this study could be extended to similar numerical models, although it may be possible that numerical models applied to condensers operating under performance conditions different from those simulated in this study, might lead to some variations in the overall behaviour.

### *Acknowledgements*

We wish to express our gratitude to the Scientific and Technological Research Organisation (FICYT), and to the company Hidroeléctrica del Cantábrico S.A. for their financial support under grants PA-TDI96-01 and PC-TDI98-01, which made this research work possible.

## REFERENCES

[1] Heat Exchange Institute, Standards for Steam Surface Condensers, 9th edition, Heat Exchange Institute, Inc., Ohio, USA, 1995.

[2] Al-Sanea S.A., Rhodes N., Tatchell D.G., Wilkinson T.S., A computer model for detailed calculation of the flow in power station condensers, I. Chem. E. Symposium Series 75 (1983) 70–88.

[3] Al-Sanea S.A., Rhodes N., Wilkinson T.S., Mathematical modelling of two-phase condenser flows, in: The Second Int. Conf. on Multi-phase Flow, London, UK, 1985, pp. 169–182.

[4] Jureidini R.H., Malin M.R., Lord M.J., Yau K.K., A three-dimensional model for power condenser design, in: The Fourth Int. PHOENICS User Conf., CHAM Ltd., Miami, USA, 1991.

[5] Malin M., Modelling flow in an experimental marine condenser, Int. Comm. Heat Mass Tran. 24 (1997) 597–608.

[6] Ormiston S.J., Raithby G.D., Carlucci L.N., Numerical modelling of power station steam condensers. Part 1:

Convergence behaviour of finite-volume model, Numer. Heat Tran. 27 (1995) 81–102.

[7] Ormiston S.J., Raithby G.D., Carlucci L.N., Numerical modelling of power station steam condensers. Part 2: Improvement of solution behaviour, Numer. Heat Tran. 27 (1995) 103–125.

[8] Zhang C., Sousa A.C.M., Venart J., The numerical and experimental study of a power plant condenser, J. Heat Tran. 115 (1993) 435–445.

[9] Zhang C., Numerical modelling using a quasi-three-dimensional procedure for large plant condensers, J. Heat Tran. 116 (1994) 180–188.

[10] Colburn A.P., Hougen O.A., Design of cooler condensers for mixture of vapours with noncondensing gases, Ind. Engrg. Chem. 26 (1934) 1178–1782.

[11] Prieto M., Suárez I., Heat and mass transfer in a thermal cycle feedwater heater, in: Astals Coma F., Gibert Pedrosa J. (Eds.), XIII National Congress of Mech. Eng., Tarrasa, Spain, 1998, pp. 616–622.

[12] Suárez I., Prieto M., Modelling flow in closed feedwater heaters, in: Celata G.P., Di Marco P., Shah R.K. (Eds.), The Second Int. Symp. on Two-phase Flow Modelling and Experimentation, Pisa, Italy, 1999, pp. 1585–1592.

[13] McAdams W.H., Heat Transmission, 3rd edition, McGraw-Hill, 1954.

[14] Rohsenow W.H., Hartnett J.P., Ganic E.N., Handbook of Heat Transfer Fundamentals, 2nd edition, McGraw-Hill, 1985.

[15] Berman L.D., Tumarov V.A., Investigation of heat transfer during condensation of flowing steam on a horizontal tube bundle, Teploenergetika 9 (10) (1962) 77–83.

[16] Taborek J., Heat Exchanger Design Handbook, Hemisphere, New York, 1983.

[17] Ackerman G., Wärmeübergang und Molekulare Stoffübertragung in Gleichen Feld Bue Grossen Temperatur und Partialdruckdifferenzen, Forschungsheft 382 (1937).